Chinese Physics B

PAPER

Spin glassy behavior and large exchange bias effect in cubic perovskite $Ba_{0.8}Sr_{0.2}FeO_{3-\delta}$*

To cite this article: Yu-Xuan Liu *et al* 2019 *Chinese Phys. B* **28** 068104

Spin glassy behavior and large exchange bias effect in cubic perovskite $Ba_{0.8}Sr_{0.2}FeO_{3-\delta}$*

Yu-Xuan Liu(刘宇轩)[1,2], Zhe-Hong Liu(刘哲宏)[2,3], Xu-Bin Ye(叶旭斌)[2,3], Xu-Dong Shen(申旭东)[2,3], Xiao Wang(王潇)[2,3], Bo-Wen Zhou(周博文)[2,3], Guang-Hui Zhou(周光辉)[1,†], and You-Wen Long(龙有文)[2,4,‡]

[1] *Department of Physics and Synergetic Innovation Center for Quantum Effects and Applications of Hunan Province, Hunan Normal University, Changsha* 410081, *China*

[2] *Beijing National Laboratory for Condensed Matter Physics, Institute of Physics, Chinese Academy of Sciences, Beijing* 100190, *China*

[3] *School of Physics, University of Chinese Academy of Sciences, Beijing* 100049, *China*

[4] *Songshan Lake Materials Laboratory, Dongguan* 523808, *China*

(Received 5 March 2019; revised manuscript received 26 March 2019; published online 8 May 2019)

A single-phase iron oxide $Ba_{0.8}Sr_{0.2}FeO_{3-\delta}$ with a simple cubic perovskite structure in *Pm*-3*m* symmetry is successfully synthesized by a solid-state reaction method in O_2 flow. The oxygen content is determined to be about 2.81, indicating the formation of mixed Fe^{3+} and Fe^{4+} charge states with a disorder fashion. As a result, the compound shows small-polaron conductivity behavior, as well as spin glassy features arising from the competition between the ferromagnetic interaction and the antiferromagnetic interaction. Moreover, the competing interactions also give rise to a remarkable exchange bias effect in $Ba_{0.8}Sr_{0.2}FeO_{2.81}$, providing an opportunity to use it in spin devices.

Keywords: high-pressure synthesis, exchange bias effect, spin glass

PACS: 81.40.Vw, 75.50.Lk, 75.30.Et, 75.30.Gw **DOI:** 10.1088/1674-1056/28/6/068104

1. Introduction

Iron-based oxides with higher Fe valence states like Fe^{4+} exhibit intriguing physical properties. For example, charge disproportionation is found to occur in $CaFeO_3$ and $CaCu_3Fe_4O_{12}$,[1,2] which leads to crystal structural phase transition accompanied with metal-insulator transformation. In addition, Cu–Fe intermetallic charge transfer takes place in $RCu_3Fe_4O_{12}$ (R = La, Pr, Nd, Bi),[3–9] giving rise to a first-order isostructural phase transition and a series of sharp variations in magnetism and electrical transport properties. $BaFeO_3$ usually crystallizes into a hexagonal phase by the high-temperature anneal method in oxygen flow.[10] Recently, a simple cubic perovskite phase of $BaFeO_3$ is reported to have been prepared when a lower-temperature reaction method is adopted through using ozone as an oxidizing agent,[11] although only a limited thickness of powder sample (ca. 50 nm) can be obtained by this method.

In the 1950s, Meiklejohn and Bean[12] discovered the so-called exchange bias (EB) effect in the Co core and CoO shell structure. In general, this effect can occur when a sample is cooled in a magnetic field across the a critical temperature of a magnetic phase transition because the magnetic hysteresis will shift from the center point vertically or horizontally.[13] The EB effect promises to have potential applications in spin valves,[14] ultra high-density recording,[15] permanent magnets, *etc*.[16] Therefore, it has received much attention in many different material systems such as ferromagnetic (FM)–antiferromagnetic (AFM) bilayers,[17] nanostructured compounds (nanowires[18] and nanoparticles[19]), strongly correlated oxides,[20] heterostructures, *etc*.[21] Moreover, it is found that the competition between the FM interaction and the AFM interaction in a spin glassy system can significantly induce the EB effect.[22,23]

In this work, an oxygen deficient iron compound $Ba_{0.8}Sr_{0.2}FeO_{2.81}$ with a simple cubic perovskite structure is prepared. The random distribution of Fe^{3+} and Fe^{4+} causes competition between the FM interaction and AFM interaction, resulting in a spin glassy behavior which can be well explained by a critical slowing down model. More interestingly, a large exchange bias effect is observed in this compound.

2. Experimental details

The $Ba_{0.8}Sr_{0.2}FeO_{2.81}$ was prepared by a solid-state anneal method. The stoichiometric powders $BaCO_3$ (99.99%), $SrCO_3$ (99.99%), and Fe_2O_3 (99.99%) used as starting materials were thoroughly mixed and ground in an agate mortar. The mixture was then heated in a tube furnace at 1323 K in

*Project supported by the National Key Research and Development Program of China (Grant Nos. 2018YFA0305700 and 2018YFGH000095), the National Natural Science Foundation of China (Grant Nos. 51772324 and 11574378), and the Fund from the Chinese Academy of Sciences (Grant No. QYZDB-SSW-SLH013, GJHZ1773).

†Corresponding author. E-mail: ghzhou@hunnu.edu.cn

‡Corresponding author. E-mail: ywlong@iphy.ac.cn

O_2 flow for 24 h. The powder x-ray diffraction (XRD) was measured by a Huber diffractometer with Cu Kα_1 radiation at 40 kV and 30 mA at room temperature. The diffraction angle is selected in a range from 5° to 100° in steps of 0.05°. The XRD data were analyzed by Rietveld refinement with the GSAS program.[24] The oxygen content was evaluated by thermogravimetric (TG) analysis on a Setaram TG-DTA system. The sample was heated up to 950 K in Ar flow with a heating speed of 10 K/min. Temperature dependence of magnetic susceptibility and field dependence of magnetization were measured by using a superconducting quantum interference device magnetometer (Quantum Design, SQUID-VSM). The alternating current (ac) magnetization, specific heat, and electrical transport properties were measured on a physical property measurement system (Quantum Design, PPMS-9 T).

3. Results and discussion

Figure 1(a) shows the XRD pattern of $Ba_{0.8}Sr_{0.2}FeO_{2.81}$ measured at room temperature. The Rietveld analysis demonstrates that the compound crystallizes into a simple cubic perovskite structure with space group *Pm*-3*m*. The lattice parameter we refined is $a = 3.93943(1)$ Å. This value is slightly smaller than that of $BaFeO_3$ (~ 3.971 Å), due to the partial introduction of Sr at the A site. To identify the oxygen content, we perform TG measurement as shown in Fig. 1(b). The compound is thermally stable below ~ 550 K. Above this temperature, there exists a remarkable weight loss, indicating the occurrence of oxygen release. Above 800 K, the product becomes stable again on heating up to 950 K, the maximum temperature that is used for TG measurement. According to the TG loss, as well as the final product ($Ba_{0.8}Sr_{0.2}FeO_{2.5}$ identified by XRD), the oxygen content is determined to be 2.81 ± 0.02, suggesting the presence of a mixed $Fe^{3.62+}$ valence state. Therefore, the perovskite B site should be occupied by randomly distributed Fe^{3+} and Fe^{4+} in the current $Ba_{0.8}Sr_{0.2}FeO_{2.81}$.

Figure 2(a) shows the temperature dependence of direct current (DC) magnetic susceptibility of $Ba_{0.8}Sr_{0.2}FeO_{2.81}$ measured at 0.1 T using zero-field-cooling (ZFC) and field-cooling (FC) mode. Obviously, the ZFC curve displays a kink around 50 K. However, there is a large separation between the ZFC and FC susceptibility curves below this temperature. This feature can usually be caused by a canted long-range AFM ordering or a spin glassy effect.[25] However, when the specific heat as a function of temperature is measured (see Fig. 2(b)), one cannot find any anomaly in the whole temperature region we measured (2 K–100 K), ruling out the possibility of long-range spin ordering in $Ba_{0.8}Sr_{0.2}FeO_{2.81}$. Therefore, the compound should experience a spin glassy transition at a critical temperature $T_g \approx 50$ K. Note that the specific heat below 10 K can be well fitted by the formula $C_p = \beta T^{3/2} + \alpha T^3$. The fitting gives $\beta = 5.31 \times 10^{-3}$ J·mol^{-1}·K$^{-5/2}$, and $\alpha = 1.79 \times 10^{-4}$ J·mol^{-1}·K^{-4}, indicating that both FM interaction and AFM interaction play a role in specific heat, which is in agreement with the magnetic measurement result. As mentioned earlier, there exist random Fe^{3+} and Fe^{4+} ions in the cubic perovskite $Ba_{0.8}Sr_{0.2}FeO_{2.81}$. The 180° Fe^{3+}–O–Fe^{3+} superexchange pathways can contribute to the AFM interaction, whereas the contribution to FM can be made by the Fe^{3+}–O–Fe^{4+} double exchange. The competition between the FM interaction and the AFM interaction is thus responsible for the spin glassy behavior observed in $Ba_{0.8}Sr_{0.2}FeO_{2.81}$. Note that the field dependence of magnetization of $Ba_{0.8}Sr_{0.2}FeO_{2.81}$ presented in the inset of Fig. 2(a) is also consistent with the spin glassy feature.

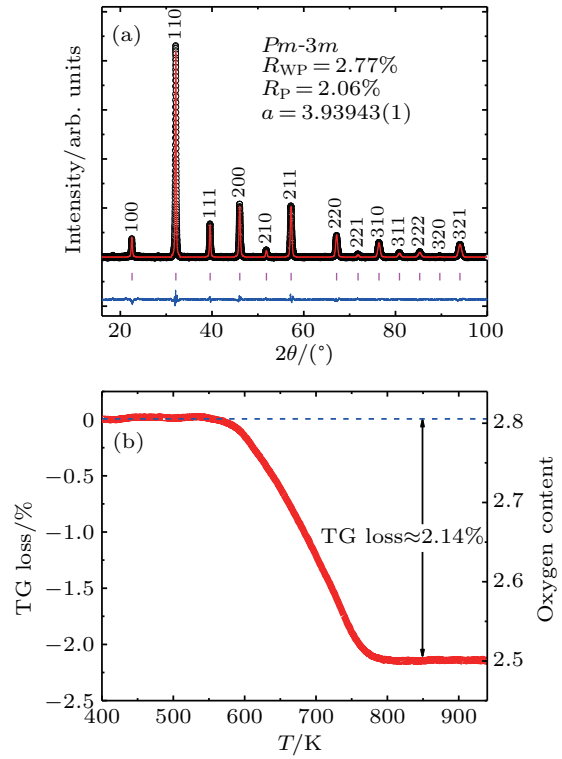

Fig. 1. (a) The XRD pattern and the Rietveld refinement result of $Ba_{0.8}Sr_{0.2}FeO_{2.81}$, where black circle and red line represent the observed and fitted data, respectively. Bottom blue line represents their difference,and pink ticks denote allowed Bragg reflections; (b) TG measurement result of $Ba_{0.8}Sr_{0.2}FeO_{2.81}$.

Figure 2(c) shows the temperature dependence of resistivity measured on a pellet of $Ba_{0.8}Sr_{0.2}FeO_{2.81}$. As the temperature decreases, the resistivity increases sharply, suggesting semiconducting or insulating electrical transport properties. Different electrical conductivity modes are attempted to fit the resistivity data. Like some manganites composed of mixed Mn^{3+} and Mn^{4+},[26,27] the hopping model of small polarons can well reproduce the electrical transport of $Ba_{0.8}Sr_{0.2}FeO_{2.81}$ in a temperature range between 250 K and 300 K. The inset of Fig. 2(c) shows the fitting result by using the function $\rho = \rho_0 T \exp(E_A/KT)$. Here the E_A represents the activation energy, and K is the Boltzman constant.

The E_A we fitted is 224 meV. This value is slightly less than that obtained from the hexagonal $BaFeO_{2.86}$ (300 meV) and $BaFeO_{2.9}$ (260 meV),[28] which is probably due to the more straight Fe–O–Fe bonding in the current $Ba_{0.8}Sr_{0.2}FeO_{2.81}$ with a cubic perovskite structure.

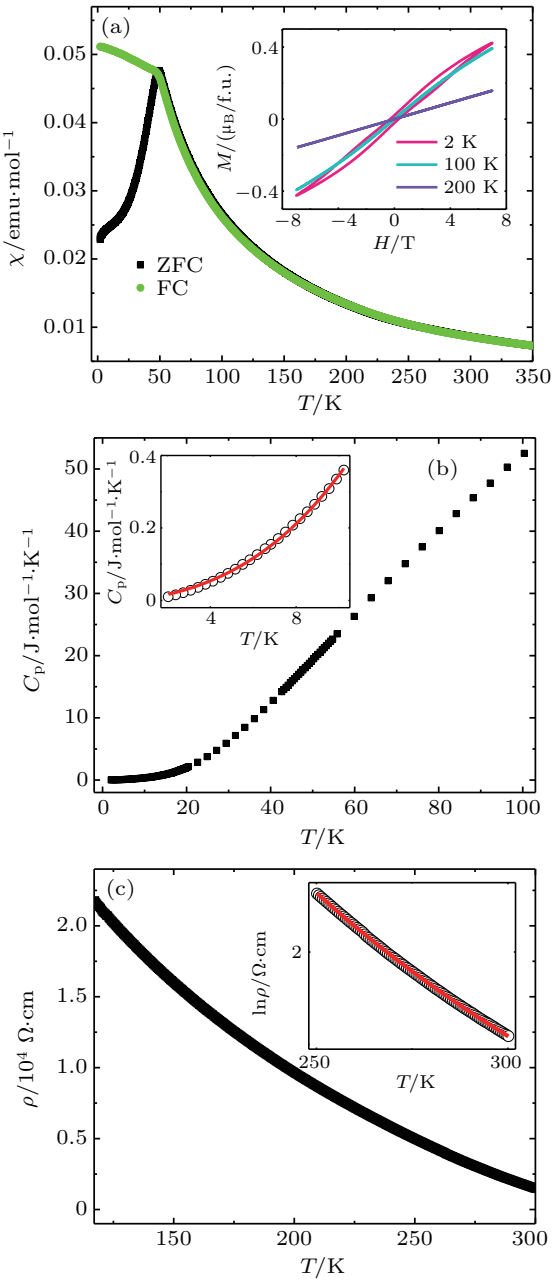

Fig. 2. (a) Plots of temperature dependence of DC magnetic susceptibility measured at 0.1 T. The inset shows plots of magnetization *versus* magnetic field, measured at different temperatures for $Ba_{0.8}Sr_{0.2}FeO_{2.81}$. (b) Temperature dependence of specific heat, measured between 2 and 100 K. Inset shows fitting result (red curve) using function $C_p = \beta T^{3/2} + \alpha T^3$. (c) Temperature dependence of resistivity. Inset shows fitting result (red line) using hopping model of small polarons as described in the text.

To further characterize the spin glassy state of $Ba_{0.8}Sr_{0.2}FeO_{2.81}$, the AC magnetization values are measured at different frequencies. As shown in Fig. 3, a frequency-dependent cusp that shifts toward higher temperatures with the increasing of frequency is found to occur near the freezing temperature T_f (see the upper-left inset), providing convincing evidence for the formation of spin glass. Moreover, the spin glassy behavior of $Ba_{0.8}Sr_{0.2}FeO_{2.81}$ can be well described by the critical slowing down model[29] with the formula $\tau_f = \tau_0(T_f/T_g - 1)^{-zv}$, where τ_0 is the relaxation time, the parameter zv is the dynamic critical exponent, and the maximum relaxation time $\tau_f = 1/f$. The bottom-right inset of Fig. 3 presents the fitting result, yielding the parameters $\tau_0 = 6.8(6) \times 10^{-14}$ s and $zv = 11.03(4)$. These values are comparable to those observed in other spin glassy systems, like $Eu_{0.4}Sr_{0.6}S$, Sr_2FeCoO_6,[30–32] *etc*.

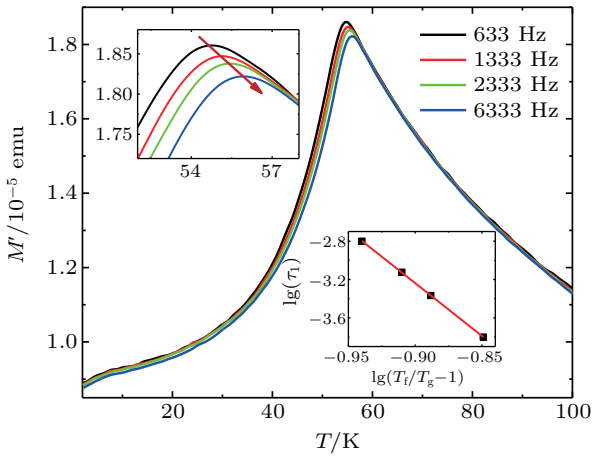

Fig. 3. Plots of AC magnetization *versus* temperature, measured between 2 K and 100 K for $Ba_{0.8}Sr_{0.2}FeO_{2.81}$. The upper-left inset shows enlarged view for the shift. Bottom right inset shows fitting by using critical slowing down model as described in the text.

Since the spin glassy behavior caused by the competition between the FM interaction and the AFM interaction is highly likely to induce a large exchange bias effect, the FC magnetization curves are measured at 2 K. For these measurements, the sample is cooled from 300 K to 2 K through the T_g under different positive cooling fields (0 T–7 T). Figure 4(a) shows the related measurement results. The asymmetrical magnetic hysteresis loops that deviate from the origin point can be well observed. Specifically, the magnetization curves shift towards the negative magnetic field axis and the positive magnetization axis, revealing the remarkable exchange bias effect. To quantitatively characterize the exchange bias effect of $Ba_{0.8}Sr_{0.2}FeO_{2.81}$, the EB field ($H_{EB} = (|H_L| - |H_R|)/2$) and the remnant magnetization shift ($M_E = (|M_U| - M_D|)/2$) are calculated. Here, the H_L and H_R respectively present the left and right cooling field intercept, and M_U and M_D are upside and downside magnetization intercept, as illustrated in the inset of Fig. 4(a), measured at a cooling field $H_{CF} = 2$ T. Figure 4(b) shows the calculated H_{EB} and M_E as a function of H_{CF}. The values of H_{EB} sharply increase at lower cooling fields ranging from 0 T to 2 T, and then gradually decrease at higher cooling fields. The maximum value of H_{EB} we obtained at 2 T is 5.6 kOe (1 Oe = 79.5775 A·m^{-1}), which is significantly higher than those for most of other compounds.[33–35]

Similarly, the M_E also sharply increases to 0.031 μ_B/f.u. with field increasing up to 2 T. Above this cooling field, it decreases slightly.

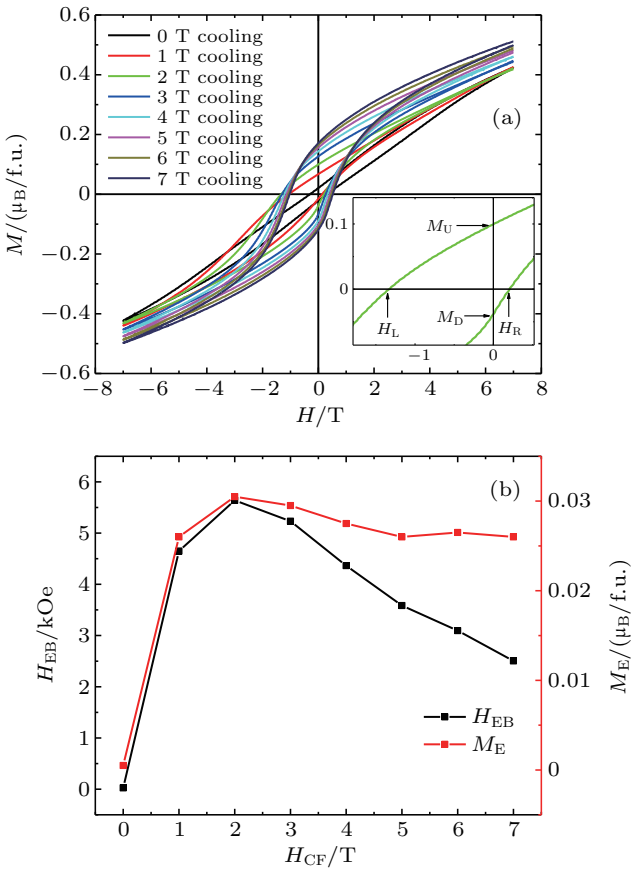

Fig. 4. (a) Plots of field dependence of magnetization measured at 2 K after cooling at different fields from 300 K to 2 K for $Ba_{0.8}Sr_{0.2}FeO_{2.81}$. Inset shows the enlarged view for the magnetic hysteresis loop measured at a 2-T cooling field. (b) Plots of H_{EB} and M_E as a function of H_{CF} obtained at 2 K.

The magnitudes of H_{EB} and M_E are dependent on factors such as FM and AFM cluster size or thickness, interfacial roughness, and exchange coupling strength between the FM interaction and the AFM interaction.[13,36–38] In the current $Ba_{0.8}Sr_{0.2}FeO_{2.81}$ composed of disordered FM and AFM domains, at $H_{CF} = 0$ T, the spin glassy state caused by the competition between the FM interaction and the AFM interaction froze at T_g. When the applied cooling field increases up to 2 T, the magnetic anisotropy sharply increases due to the pinning effect of FM domains. Consequently, the values of H_{EB} and M_E increase drastically in a cooling field range from 0 T to 2 T. Meanwhile, when the cooling field exceeds 2 T, the FM cluster size will develop considerably. Consequently, the exchange coupling effect becomes too weak to pin the FM spins, resulting in the H_{EB} and M_E decreasing at higher H_{CF}.

4. Conclusions

In summary of the present study, an oxygen deficient perovskite $Ba_{0.8}Sr_{0.2}FeO_{3-\delta}$ with simple cubic *Pm*-3*m* space group is synthesized. The oxygen content is determined to be 2.81 ± 0.02 by TG measurement. The electrical transport behavior can be well fitted by the hopping model of small polarons, and the activation energy we obtained is 224 meV. In magnetism, both DC and AC magnetic susceptibility measurements reveal the spin glassy features of $Ba_{0.8}Sr_{0.2}FeO_{2.81}$ with a glassy transition temperature at about 50 K. The spin glassy behavior can be attributed to the competition between the FM interaction and the AFM interaction originating from the Fe^{3+}–O–Fe^{4+} double exchange and Fe^{3+}–O–Fe^{3+} superexchange pathways, respectively. On using a positive magnetic field to cool $Ba_{0.8}Sr_{0.2}FeO_{2.81}$ from 300 K to 2 K through T_g, a large negative exchange bias effect is observed. Moreover, the exchange bias field increases sharply as H_{CF} increases up to 2 T, due to the FM pinning effect. The maximum H_{EB} that we obtained at 2 K is 5.6 kOe, which is located at a higher level than those observed in other compounds.

References

[1] Zhang C X, Xia H L, Liu H, Dai Y M, Xu B, Yang R, Qiu Z Y, Sui Q T, Long Y W, Meng S and Qiu X G 2017 *Phys. Rev. B* **95** 064104

[2] Lottini E, López-Ortega A, Bertoni G, Turner S, Meledina M, Van Tendeloo G, de Julián Fernández C and Sangregorio C 2016 *Chem. Mater.* **28** 4214

[3] Shimakawa Y 2015 *J. Phys. D: Appl. Phys.* **48** 504006

[4] Yamada I, Etani H, Tsuchida K, Marukawa S, Hayashi N, Kawakami T, Mizumaki M, Ohgushi K, Kusano Y, Kim J, Tsuji N, Takahashi R, Nishiyama N, Inoue T, Irifune T and Takano M 2013 *Lnorg Chem.* **52** 13751

[5] Etani H, Yamada I, Ohgushi K, Hayashi N, Kusano Y, Mizumaki M, Kim J, Tsuji N, Takahashi R, Nishiyama N, Inoue T, Irifune T and Takano M 2013 *J. Am. Chem. Soc.* **135** 6100

[6] Long Y W, Hayashi N, Saito T, Azuma M, Muranaka S and Shimakawa Y 2009 *Nature* **458** 60

[7] Wang X, Liu M, Shen X D, Liu Z H, Hu Z W, Chen K, Ohresser P, Nataf L, Baudelet F, Lin H J, Chen C T, Soo Y L, Yang Y F, Jin C Q and Long Y W 2019 *Inorg Chem.* **58** 320

[8] Long Y W and Shimakawa Y 2010 *New. J. Phys.* **12** 063029

[9] Long Y W 2016 *Chin. Phys. B* **25** 078108

[10] Mori S 1966 *J. Am. Ceram. Soc.* **49** 600

[11] Hayashi N, Yamamoto T, Kageyama H, Nishi M, Watanabe Y, Kawakami T, Matsushita Y, Fujimori A and Takano M 2011 *Angew. Chem. Int. Ed.* **50** 12547

[12] Meiklejohn W H and Bean C P 1956 *Phys. Rev.* **102** 1413

[13] Kiwi and Miguel 2001 *J. Magn. Magn. Mater.* **234** 584

[14] Jiang Y, Abe S, Ochiai T, Nozaki T, Hirohata A, Tezuka N and Inomata K 2004 *Phys. Rev. Lett.* **92** 167204

[15] Skumryev V, Stoyanov S, Zhang Y, Hadjipanayis G, Givord D and Nogués J 2003 *Nature* **423** 850

[16] Nogués J and Schuller I K 1999 *J. Magn. Magn. Mater.* **192** 203

[17] Jungblut R, Coehoorn R, Johnson M T, aan de Stegge J and Reinders A 1994 *J. Appl. Phys.* **75** 6659

[18] Salabaş E L, Rumplecker A, Kleitz F, Radu F and Schüth F 2006 *Nano. Lett.* **6** 2977

[19] de Azevedo Filho J B, de Araújo J H, Morales M A, Firme C L and de Oliveira J B 2019 *J. Magn. Magn. Mater.* **471** 177

[20] Tang Y k, Sun Y and Cheng Z h 2006 *J. Appl. Phys.* **100** 023914

[21] Chu Y H, Martin L W, Holcomb M B, Gajek M, Han S J, He Q, Balke N, Yang C H, Lee D, Hu W, Zhan Q, Yang P L, Fraile R A, Scholl A, Wang S X and Ramesh R 2008 *Nat. Mater.* **7** 478

[22] Gruyters M 2005 *Phys. Rev. Lett.* **95** 077204

[23] Ding J F, Lebedev O I, Turner S, Tian Y F, Hu W J, Seo J W, Panagopoulos C, Prellier W, Van Tendeloo G and Wu T 2013 *Phys. Rev. B* **87** 054428
[24] Toby B 2001 *J. Appl. Crystallogr.* **34** 210
[25] Mydosh J A 2014 *Spin Glasses* (London)
[26] Sun Y, Xu X J, Zhang Y H 2000 *J. Phys.: Condens. Matter* **12** 10475
[27] Goodenough J B and Zhou J S 1997 *Nature* **386** 229
[28] Hombo J, Matsumoto Y and Kawano T 1990 *J. Solid State Chem.* **84** 138
[29] Venkateswarlu B, Hari K R, Arout C J, Babu P D and Harish K N 2019 *J. Alloys Compd.* **777** 373
[30] Souletie J and Tholence J L 1985 *Phys. Rev. B.* **32** 5169
[31] Pradheesh R, Nair H S, Kumar C M N, Lamsal J, Nirmala R, Santhosh P N, Yelon W B, Malik S K, Sankaranarayanan V and Sethupathi K 2012 *J. Appl. Phys.* **111** 053905
[32] Yang J, Dai J, Liu Z, Yu R, Hojo H, Hu Z, Pi, Tunwen, Soo Y L, Jin C Q, Azuma M and Long Y W 2017 *Inorg Chem.* **56** 11676
[33] Guo Y, Shi L, Zhou S, Zhao J, Wang C, Liu W and Wei S Q 2013 *J. Phys. D: Appl. Phys.* **46** 175302
[34] Luo W J and Wang F W 2007 *Appl. Phys. Lett.* **90** 162515
[35] Karmakar S, Taran S, Bose E, Chaudhuri B K, Sun C P, Huang C L and Yang H D 2008 *Phys. Rev. B* **77** 144409
[36] Stiles M D and McMichael R D 2001 *Phys. Rev. B* **63** 064405
[37] Dong S, Yamauchi K, Yunoki S, Yu R, Liang S, Moreo A, Liu J M, Picozzi S and Dagotto E 2009 *Phys. Rev. Lett.* **103** 127201
[38] Evans R F L, Bate D, Chantrell R W, Yanes R and Chubykalo-Fesenko O 2011 *Phys. Rev. B* **84** 092404